Malaysian Journal of Chemistry, 2024, Vol. 26(6), 136-149

The Conductivity Behaviour of Acid-Doped PANI and its Effect on the Corrosion of Mild Steel in HCl

Norshahira Zainuddin and Amirah Amalina Ahmad Tarmizi*
Faculty of Applied Sciences, University Technology MARA, 40450 Shah Alam, Selangor, Malaysia
*Corresponding author (e-mail: amirahamalina@uitm.edu.my)

This study investigates how dopant acids affect the properties and electrical conductivity of polyaniline (PANI), and addresses the gap in understanding the conductivity behaviour of PANI-doped acids and their effects on the corrosion of mild steel in HCl. PANI was synthesized by chemical oxidative polymerization using sulfuric acid (SA) and oxalic acid (OA), with ammonium persulfate as the oxidant. Characterization via FTIR and SEM revealed successful doping, as indicated by the appearance of new bands in the conductive polymer and the disappearance of the aniline N-H signal at the 3500 to 3200 cm^{-1} frequency range. Morphological analysis showed that higher concentrations of dopants offered more consistent, smooth and efficient corrosion protection for mild steel. Corrosion performance was assessed using weight loss measurements, and conductivity was analysed by electrochemical impedance spectroscopy (EIS). The results demonstrated that higher concentrations of dopants significantly enhanced conductivity, with SA and OA showing values of 1.015×10^{-3} S/cm and 330×10^{-3} S/cm, respectively. PANI doped with 0.1 M OA exhibited the highest inhibitor efficiency (IE) of 15.41 %. The formation of a passive oxide layer likely contributed to lower IE percentages. EIS, conducted to analyse the inhibitor's effects on corrosion, indicated that the protection provided by PANI-doped acids was due to the passive oxide layer, as evidenced by higher impedance values and two capacitive loops after 72 hours.

Keywords: Polyaniline (PANI); conductivity; dopants (acid); inhibitor; corrosion

Received:July 2024; Accepted: September 2024

The corrosion of metals and alloys is a significant threat to industry that causes immense economic losses and casualties [1]. Corrosion, also known as rust, is an unwanted phenomenon that degrades the lustre and beauty of materials while reducing their duration of use [2]. In chemical terms, it is the process of depositing oxide, sulphide, or chloride on a material's surface. This process occurs spontaneously, without any external factors such as catalysts, temperature, or energy; corrosion occurs wherever there is moisture. However, corrosion is a slow process; it takes a long time, sometimes years, depending on the strength of the inhibitor used. An inhibitor of corrosion acts to prevent metals and alloys from corroding in different corrosive media. Inhibitors protect metal surfaces by forming protective films on the surface, preventing electrochemical reactions that cause corrosion. One class of inhibitors that can be used to prevent corrosion are conductive polymers.

Extensive research has been conducted on the effectiveness of utilizing conducting polymers, including polyaniline (PANI), polypyrrole (PPy), and polythiophene (PTH), as corrosion inhibitors due to their exceptional electrical and electronic properties [3]. These polymers typically possess conjugated backbones that exhibit electron donor-acceptor properties following oxidation or reduction [4]. Among these polymers, PANI has garnered significant attention in recent years due to its chemical stability, unique electrical properties, and ease of synthesis. The electrical conductivity of PANI can be enhanced using the doping technique, and its properties are highly dependent on the dopant acid [5]. Additionally, PANI's conductivity can be increased by treatment with acids, with the dopant acid playing a crucial role in determining its properties [6].

Dopant agents are widely used in the synthesis of conductive polymers, especially for PANI, which has proven its potential as an inhibitor of corrosion. In the synthesis of polyanilines, sulfuric and oxalic acids serve as dopant agents due to their distinct characteristics and effects on the polymer's properties. Sulfuric acid enhances the electrical conductivity of PANI by protonating the amine groups, whereas oxalic acid impacts the kinetics of polymerization, yield, electrical conductivity, solubility, and hydrophilicity of the polymer.

Previous studies have extensively utilized PANI as a protective coating to combat corrosion. Due to the majority of researchers concentrating on PANI as a protective coating, only a few studies have focussed on corrosion inhibitors involving the electrical properties of PANI dopants with mild corrosion

resistance in HCl solution. Nonetheless, there are several reports on PANI dopants. One such study by Rahman et al. (2021) explored the enhancement of electrical properties in metal-doped PANI through different doping techniques [7]. However, there remains a significant dearth of scientific research on the influence of the electrical properties of PANI-doped acids on the corrosion of mild steel in HCl.

Hence, this study aims to examine the impact of conductivity behaviour on the corrosion performance of PANI when doped with sulfuric and oxalic acids. PANI was prepared by chemical oxidative polymerization. Two different acids, sulphuric acid and oxalic acid, were used as dopants in this study. The corrosion performance of the doped PANI was tested using the weight loss method. The corrosion behaviour of all samples was also analysed using electrochemical impedance spectroscopy.

EXPERIMENTAL

Chemicals and Materials

Sigma-Aldrich supplied the aniline solution and 1-methyl-2-pyrrolidinone, while Chemiz supplied the ammonium persulfate ($(NH_4)_2S_2O_8$), APS), sulfuric acid (H_2SO_4), hydrochloric acid (HCl), and oxalic acid (OA). These chemicals were required for the synthesis of polyaniline and were not subjected to further purification. All selected chemicals were of the highest analytical grade. Distilled water was used in the preparation of aqueous solutions as well as in washing procedures.

Instruments

Using Attenuated Total Reflectance-Fourier Transform Infrared (ATR-FTIR) spectroscopy, the functional groups in the range of 4000–650 cm^{-1} were recorded at room temperature with a Perkin Elmer FTIR. The morphology was determined using a Hitachi TM3030 tabletop scanning electron microscope (SEM). Additionally, electrochemical impedance spectroscopy (EIS) studies were carried out using the Gamry 620 potentiostat model.

Preparation of Polyaniline

Polyaniline doped with sulfuric and oxalic acids was synthesized through chemical oxidative polymerization of aniline in a solution containing both acids at concentrations of 0.1 M (PANI-OA 0.1 M) and 0.08 M (PANI-OA 0.08 M), utilizing APS as the oxidizing agent. A mixture of 200 ml of 0.1 M oxalic acid and 2 mL of aniline was prepared in a beaker, while in another, APS was dissolved in 50 mL of distilled water. The oxidant was then added dropwise to the aniline mixture under ice-bath conditions with continuous stirring. After 6 hours of stirring, the mixture was refrigerated overnight for the aging process. The resulting product was filtered using a vacuum filter and thoroughly washed with distilled water. The dark green precipitate, polyaniline doped oxalic acid (PANI-OA), was subsequently dried overnight in an oven at 60 °C [7]. The same method was used to prepare polyaniline doped with sulfuric acid (PANI-SA) with the same concentrations at 0.1M and 0.08 M.

Characterization Methods

Two techniques were used in this study to characterize the prepared PANI, namely SEM and ATR-FTIR. The morphology of the metal surface was studied using SEM, while the functional groups in the synthesised PANI were analysed by ATR-FTIR in the region of 4000 cm^{-1} to 650 cm^{-1}.

SEM images were obtained at 10,000x magnification to examine the surface morphology of the PANI sample. For the ATR-FTIR analysis, the sample was placed in a holder in front of the IR source. The signal was converted to a spectrum by a detector after being read in analogue format. Signal analysis and peak identification were performed by a computer.

Weight Loss

Using the weight loss approach, the inhibition capacity of the PANI dopant was assessed at different operational times. Sandpaper was used to polish 1 cm × 1 cm mild steel (MS) coupons before each experiment. The specimens were then precisely weighed. Following that, the coupons were immersed in electrolytes, 0.5 M HCl + PANI-OA and 0.5 M HCl + PANI-SA. After specific immersion periods (1, 6, 24, 48, 72 hours), the specimens were removed, washed with distilled water, and weighed once again. This method was used to calculate the average weight loss (WL), corrosion rate (CR), and corrosion inhibition efficiency (IE%). The calculation of the data used the following formula:

$$\mathrm{CR} = \frac{(\mathrm{K} \times \mathrm{WL})}{(\mathrm{A} \times \mathrm{T} \times \mathrm{p})} \quad (1)$$

where WL stands for mass loss in grams, A for metal area in cm^2, T for exposure time in hours, and p for metal density in grams per cm^3. K is a constant of 8.76×10^4 (in mm/year).

$$IE\% = \frac{W2 - W1}{W2} \times 100 \quad (2)$$

where W1 is the weight loss with the inhibitor, while W2 is the weight loss without the inhibitor.

Electrochemical Impedance Spectroscopy (EIS)

Electrochemical impedance spectroscopy (Gamry 620 potentiostat) was used to understand the corrosion mechanism of PANI. A three-electrode corrosion system was used to measure EIS, where the working electrode was mild steel, the reference electrode was graphite, and the counter electrode was silver chloride. This procedure was carried out at room temperature, in the frequency range of 100 kHz to 0.01 Hz. The PANI-infused samples were clipped with mild steel (1 cm^2) disc electrodes. To determine the current flowing through the sample, EIS utilized a small sinusoidal wave of 10 mV at room temperature. The impedance at each operating frequency was recorded. The inhibition efficiency value (IE%) was calculated from the R_{ct} value using the following equation:

$$IE\% = \frac{R^{\circ}_{ct} - R_{ct}}{R^{\circ}_{ct}} \times 100 \quad (3)$$

where R°_{ct} and R_{ct} are the charge transfer resistance values in the absence and presence of the inhibitor.

RESULTS AND DISCUSSION

Fourier Transmission Infrared (FTIR) Spectroscopy

According to Shah & Ul Haq (2022), FT-IR spectroscopy is an effective way to determine structural composition [1]. This study utilized ATR-FTIR to analyse the structures of PANI with various acid dopants and concentrations.

Figure 1 shows three distinct samples, aniline, pure oxalic acid, and 0.1 M oxalic acid doped with polyaniline. The successful polymerization of aniline is suggested by the disappearance of two N-H stretching peaks in the PANI spectrum related to the primary amine of aniline in the range of 3500 to 3200 cm^{-1}. The peaks in doped PANI at 1564 cm^{-1} were ascribed to the quinoid ring, whereas the peak at 1485 cm^{-1} was caused by the characteristic C=C bonds of the benzene ring. On the other hand, the quinone ring's C-N stretching peak was observed at 1300 cm^{-1} [3]. This band is directly related to electrical conductivity and is linked to the polaron structure that arises upon doping. The peak at 1247 cm^{-1} was associated with the polymer structure's C-O stretching vibration. This result clearly shows that the doping process was successful, and that a new material with a unique structure and chemical bonds was produced.

The FTIR spectra of the PANI samples doped with 0.1 M and 0.08 M oxalic acid are shown in Figure 2, while the associated peaks of the spectra are listed in Table 1. This provides details of the functional group and type of bonding based on their corresponding wavenumbers, which allows us to make a comparison between these two concentrations of PANI doped with oxalic acid. As we can see from the spectra, there was a slight shift in the quinoid ring C=C stretching vibrations, which showed a prominent peak at 1564 cm^{-1} for PANI-OA 0.1 M and 1566 cm^{-1} for PANI-OA 0.08 M. This slight shift revealed a small variation in the quinoid structure that was affected by the concentration of oxalic acid. These resemble the C=C stretching of benzenoid rings. There was only a slight difference between the peaks in the spectra of PANI-OA 0.1 M and PANI-OA 0.08 M, located at 1485 cm^{-1} and 1487 cm^{-1} respectively. The peaks in this region were due to the presence of oxalate ions in the PANI structure [8].

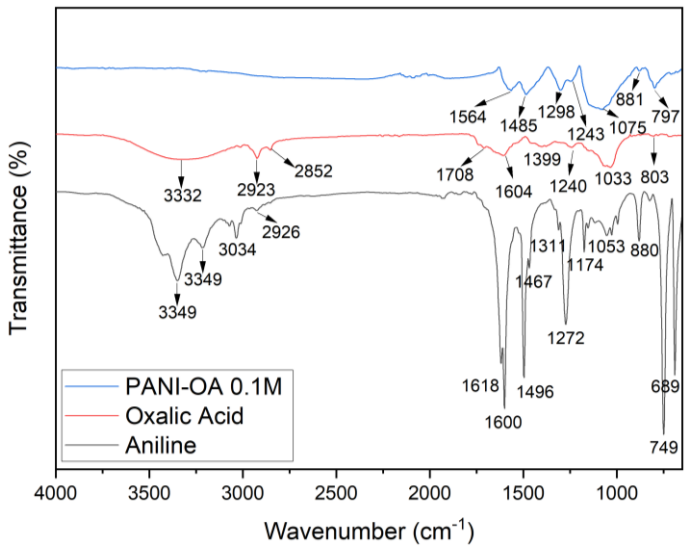

Figure 1. Infrared spectra of aniline, oxalic acid and PANI-OA 0.1 M.

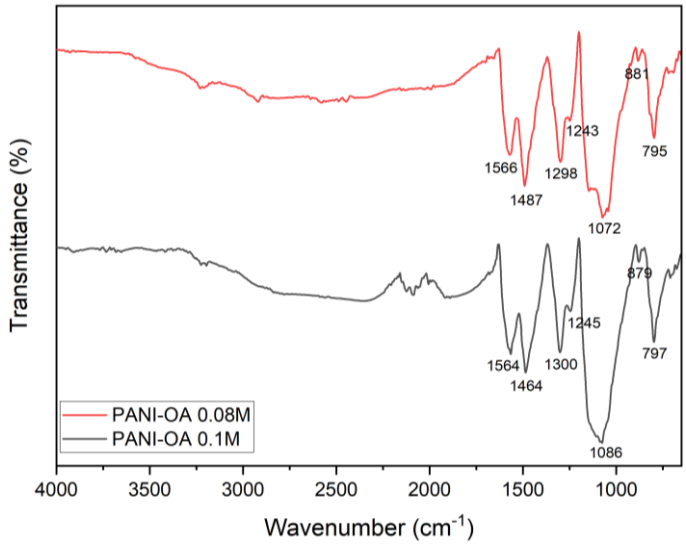

Figure 2. Infrared spectra of PANI doped with oxalic acid at 0.1 M and 0.08 M.

Table 1. The peaks associated with Figure 2.

Wavenumber			
PANI-OA 0.1 M	PANI-OA 0.08 M	Compound	Bonding
1564	1566	Amine	C=C Stretching (Quinoid ring)
1464	1487	Amine	C=C Stretching (Benzene ring)
1300	1298	Aromatic ring	C-H Bending
1245	1243	Amine	C-N Stretching
1086	1072	Carboxylic acid	C-O Stretching
879,797	881,795	Aromatic ring	C-H Bending (out-of-plane)

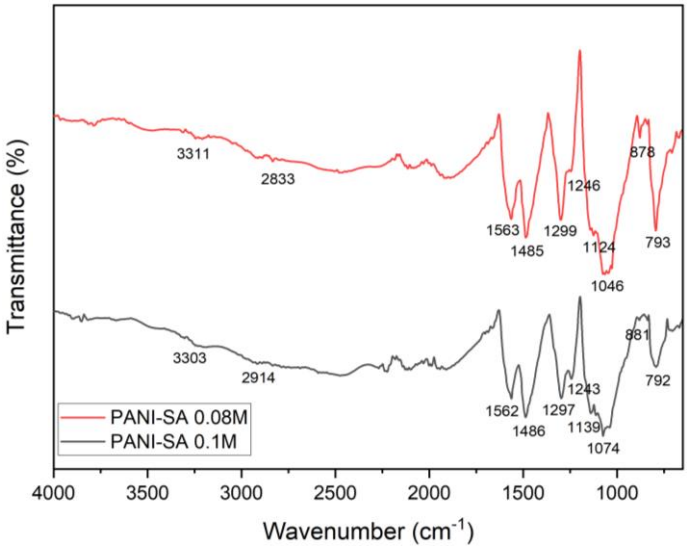

Figure 3. Infrared spectra of PANI doped with sulfuric acid at 0.1 M and 0.08 M.

The existence of C-N stretching, indicated by peaks at 1245 cm^{-1} and 1243 cm^{-1} in the PANI-OA 0.1 M and PANI-OA 0.08 M spectra, respectively, suggests the presence of an amine group. The conductivity behaviour of polyaniline is associated with this peak [8]. The PANI-OA 0.1 M sample showed a peak at 1086 cm^{-1}, while the PANI-OA 0.08 M sample showed a peak at 1072 cm^{-1}, both of which are characteristic of C-O stretching for carboxylic acid groups. The presence of a peak at 1072 cm^{-1} to 1086 cm^{-1} is indicative of the interaction between the PANI chains and the dopant molecules. The peak for PANI-OA 0.08 M at 1072 cm^{-1} shifted to a higher value and was more intense when PANI was doped with a higher

concentration of oxalic acid. The out-of-plane C-H bending vibrations of the aromatic ring can be observed at 879 cm^{-1} and 797 cm^{-1} for the PANI-OA 0.1 M sample, and at 880 cm^{-1} and 795 cm^{-1} for the PANI-OA 0.08 M sample [9].

Figure 3 and Table 2 provide details of the spectra of PANI doped with sulfuric acid at 0.1 M and 0.08 M. An N-H stretching vibration of aromatic amines can be seen at 3303 cm^{-1} in the IR spectrum of PANI doped with 0.1 M sulfuric acid, and at 3311 cm^{-1} in the IR spectrum of PANI doped with 0.08 M sulfuric acid. These similarities imply that the primary amine groups in the polyaniline structure remained at both doping concentrations [10]. Also, the C-H stretching vibrations of the aromatic and aliphatic groups were observed at 2914 cm^{-1} in PANI-SA 0.1 M and 2833 cm^{-1} in PANI-SA 0.08 M [10]. The shift demonstrates the hydrogen bonding environment, which is slightly different depending on the sulfuric acid concentration. C=C stretching vibrations of the quinoid and benzenoid rings were visible in the spectra. These peaks were detected at 1562 cm^{-1} and 1486 cm^{-1} for PANI-SA 0.1 M, while those for PANI-SA 0.08 M were located at 1563 cm^{-1} and 1485 cm^{-1}. The presence and similarity of these peaks in both spectra confirmed that the conjugated structure of polyaniline was maintained.

The aromatic ring C-H bending vibrations were also observed at 1299 cm^{-1} and 1297 cm^{-1} in PANI-SA 0.08 M and PANI-SA 0.1 M, respectively. The presence of the characteristic C-N stretching of aromatic amines can be seen at 1243 cm^{-1} in PAN-SA 0.1 M and 1246 cm^{-1} in PANI-SA 0.08 M. Their identical appearance proves that at both doping concentrations, the amine groups in the polymer structure remained. S=O stretching was responsible for two peaks, one at 1139 cm^{-1} in PANI-SA 0.1 M and another at 1124 cm^{-1} in PANI-SA 0.08 M. These peaks showed the presence of sulfuric acid doping. Out-of-plane C-H bending vibrations for aromatic rings were displayed in the PANI-SA 0.08 M spectrum at 878 cm^{-1} and 793 cm^{-1}. In the PANI-SA 0.1 M spectrum, these peaks were observed at 881 cm^{-1} and 792 cm^{-1}.

However, the intensity of the absorption peaks at 1243 cm^{-1} (PANI-SA 0.1 M) and 1246 cm^{-1} (PANI-SA 0.08 M) correspond to the conductivity behaviour and can be verified by correlating them with conductivity data. The peak at 1243 cm^{-1} for PANI-SA 0.1 M was more intense compared to that of PANI-SA 0.08 M at 1246 cm^{-1}. According to the conductivity data, a higher concentration was associated with a higher conductivity value. As opposed to lower concentrations at the quinoid and benzenoid ring peaks, the FTIR results indicated that higher concentrations of both acid dopants had broader peaks, and a slight shift was observed.

Conductivity of Doped Polyaniline

Conductivity (σ) is the ratio of current density to electric field strength and indicates a material's capacity to conduct electrons. Examining how dopants affect PANI's electrical characteristics was one of the study's major objectives. In this conductivity test, 1-methyl-2-pyrrolidinone served as the solvent, combined with a 3 % inhibitor. The conductivity values for the PANI samples used in this study are listed in Table 3.

Table 2. The peaks associated with Figure 3.

Wavenumber			
PANI-SA 0.1 M	PANI-SA 0.08 M	Compound	Bonding
3303	3311	Amine	N-H Stretching
2914	2833	Aromatic	C-H Stretching
1562	1563	Amine	C=C Stretching (Quinoid ring)
1486	1485	Amine	C=C Stretching (Benzenoid ring)
1297	1298	Aromatic ring	C-H Stretching
1243	1246	Amine	C-N Stretching
1139	1124	Sulfur-oxygen	S=O Stretching
1074	1046	Aromatic ring	C-H Stretching
881,792	878,793	Aromatic ring	C-H Bending (out-of-plane)

Table 3. Conductivity of doped PANI samples.

Doped PANI	**pH**	**Conductivity (S/cm)**
PANI-OA 0.1 M	4.39	$330 \times 10^{-3} \pm 0.5$
PANI-OA 0.08 M	4.09	$1.063 \times 10^{-3} \pm 0.5$
PANI-SA 0.1 M	3.60	$1.015 \times 10^{-3} \pm 0.5$
PANI-SA 0.08 M	3.18	$0.690 \times 10^{-3} \pm 0.5$

An overview of the conductivity changes seen in PANI samples doped with various acids at different concentrations is given in Table 3. The performance of PANI was significantly influenced by conductivity, which measures a material's capacity to conduct electricity. Acid doping is a widely used technique to introduce charge carriers and improve conductivity. Among the samples, PANI that was doped with 0.1 M OA exhibited the highest conductivity of 330×10^{-3} S/cm and pH of 4.39, while it significantly decreased to 1.063×10^{-3} S/cm and pH 4.09 at 0.08 M. The FTIR results also supported the conductivity behaviour of PANI-OA. The conductivity behaviour of PANI-OA can be seen at 1074–1075 cm^{-1} in the FTIR spectra. A shift to a lower wavenumber (1074 cm^{-1} for PANI-OA 0.1M) and a more intense peak indicate a greater degree of electron delocalization. This is probably because the dopant and polymer chains interact better, which increases the mobility of the charge carriers. Since there are more charge carriers available for movement through the polymer matrix, higher mobility increases conductivity [11]. This may be due to the higher conductivity behaviour of PANI-OA 0.1 M. The SEM results indicated a more porous structure for PANI-OA 0.1 M, which may also contribute to the higher conductivity of this sample. Porous structures enhance a material's conductivity by allowing a greater surface area for charge transfer [12]. This indicates that higher dopant concentration and pH lead to better conductivity for OA-doped PANI.

SA-doped PANI samples also showed reduced conductivity, roughly 1.015×10^{-3} S/cm (pH 3.60) and 0.690×10^{-3} S/cm (pH 3.18), respectively, at concentrations of 0.1 M and 0.08 M. This result was supported by the FTIR spectra where the conductivity behaviour could be observed at 1074 cm^{-1} - 1046 cm^{-1}. The peak for PANI-SA 0.1 M was more intense and had shifted to a lower region (1074 cm^{-1}), due to the greater conductivity of PANI-SA 0.1 M compared to PANI-SA 0.08 M. The trend observed for sulfuric acid was consistent with that of oxalic acid, where a higher dopant concentration and pH corresponded to higher conductivity. This finding agrees with a previous study [13].

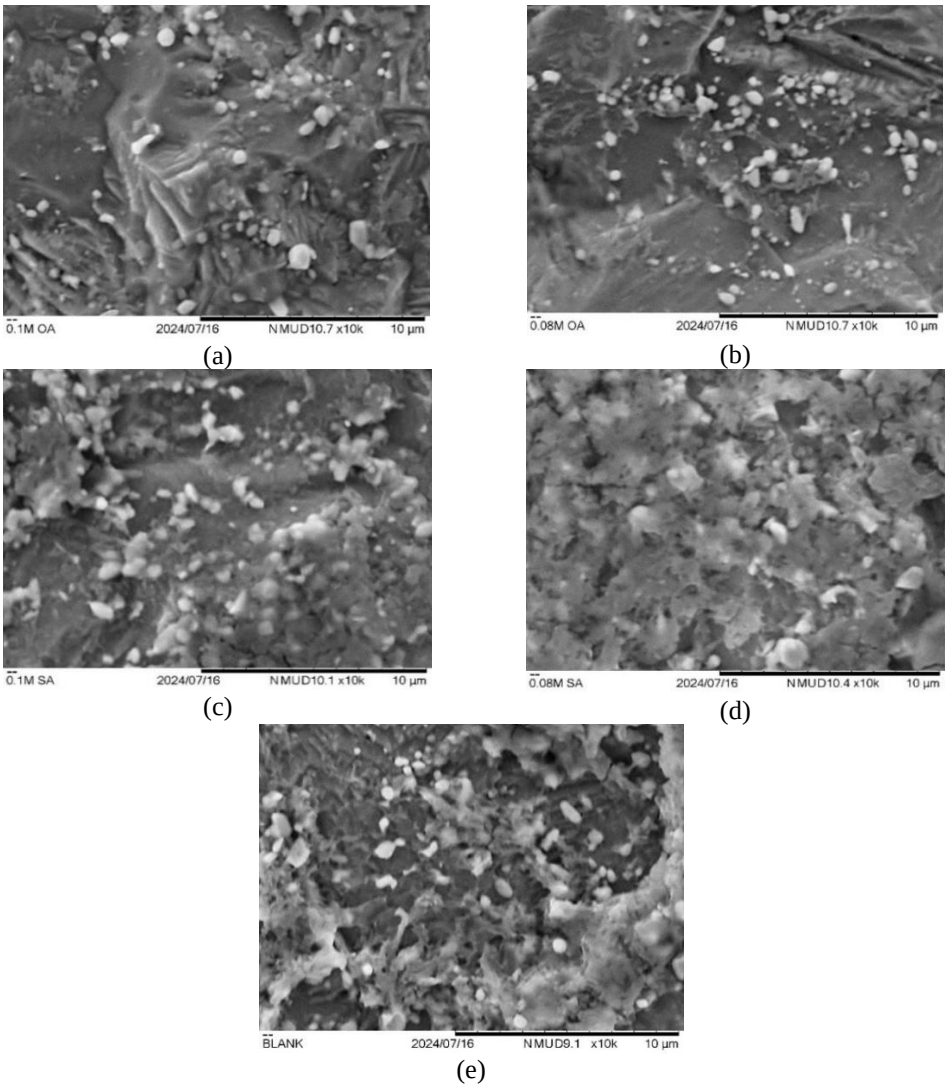

Figure 4. Morphology of the metal surfaces with and without an inhibitor at 10,000x magnification: (a) PANI-OA 0.1 M, (b) PANI-OA 0.08 M, (c) PANI-SA 0.1 M, (d) PANI-SA 0.08 M, (e) Blank.

In summary, the data in Table 3 illustrates that higher concentrations and pH values typically correlate with better conductivity in both oxalic and sulfuric acid-doped PANI. These findings are supported by the FTIR and SEM results, which showed that PANI-OA 0.1 M (1074 cm^{-1}) and PANI-SA 0.1 M (1074 cm^{-1}) had higher conductivity values due to the more intense and lower wavenumber peaks in their FTIR spectra, and the more porous structures visible in their SEM images. However, Goswami et al. (2023) suggested that extremely low pH levels, especially for sulfuric acid, can lead to greater conductivity [13]. This comparison highlights the significance of pH and acid type in determining the conductivity of doped PANI samples.

SEM Study

Figure 4 depicts the morphological images of the metal surfaces in the absence and presence of inhibitors. The images were obtained 72 hours after immersion, which was the optimal period based on the weight loss results. The figure clearly shows that the type of dopant and its concentration affected the morphology of the samples. The surface morphology of the higher concentration acid-doped PANI samples, (a) PANI-OA 0.1 M and (c) PANI-SA 0.1 M, was relatively smooth with fewer and smaller particle agglomerates, indicating uniform and effective inhibition provided by both acids at higher concentrations. Acid-doped PANI with lower concentrations showed slightly less homogeneity and rougher textures, respectively, as can be observed in (b) PANI-OA 0.08 M and (d) PANI-SA 0.08 M. This trend indicates that a uniform surface in PANI doped with acids at higher concentrations can enhance the effectiveness of inhibitors against corrosion, compared to PANI doped with acids at lower concentrations which resulted in a slightly rougher surface. However, for the blank sample (e) (mild steel in 0.5 M HCl without an inhibitor), the surface was rougher and more irregular due to the absence of an inhibitor on the metal surface. This roughness proves that the lack of a protection layer made the surface more susceptible to corrosion. Thus, these findings can be correlated with the conductivity, weight loss analysis, and morphology data of the doped PANI samples, which lead to the same conclusion, that PANI doped with acids at higher concentrations had the best conductivity and efficiency. The morphology of the doped PANI samples also showed that PANI doped with higher concentrations of acids were more porous compared to PANI doped with lower concentrations of acids.

Weight Loss Analysis

Weight loss analysis is a popular gravimetric method for measuring corrosion because of its simplicity and reliability. This analysis was performed at room temperature in a 0.5 M hydrochloric acid medium. The average weight loss, corrosion rate, and inhibition efficiency values for each experiment are recorded in Table 4.

The average weight loss of each sample over its immersion period is shown in Figure 5. It also reveals the differences between the samples with and without an inhibitor. All samples showed a weight loss trend that gradually increased with longer immersion times. The blank sample had the highest weight loss due to natural degradation and the absence of an inhibitor in the acid solution. Comparatively, the samples that contained inhibitors (PANI-OA and PANI-SA), had significantly lower weight loss than the blank samples. A reduction in weight loss suggests that the corrosion process is retarded by the inhibitor. Moreover, the weight loss in PANI-OA 0.1 M was lower compared to PANI-OA 0.08 M. The same trend was observed for PANI-SA, where for PANI doped with a higher concentration of acid, PANI-SA 0.1 M, the weight loss was reduced compared to PANI doped with 0.08 M sulfuric acid (PANI-SA 0.08 M).

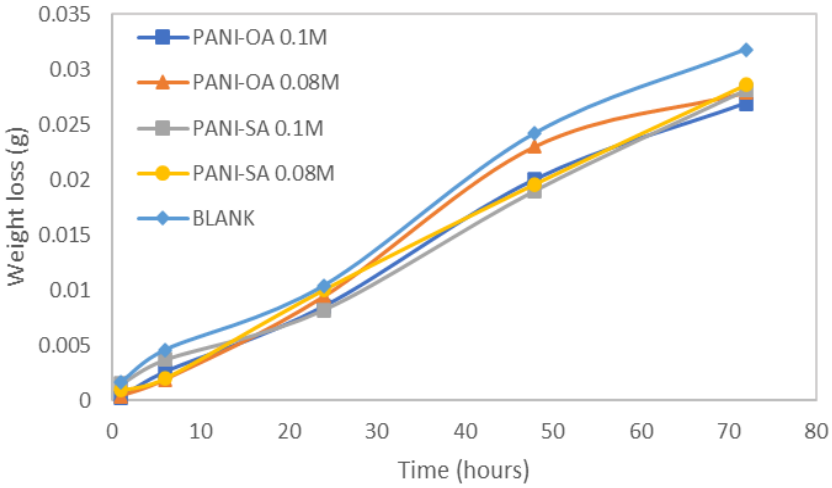

Figure 5. Weight loss vs. immersion time for all samples.

This demonstrated how the efficiency of the inhibitor increased with concentration. The resulting trend was consistent with the results of Lu et al. (2022), which also suggested that the corrosion performance of an inhibitor improved with its concentration [3]. This is because the inhibitor molecules attach themselves to the mild steel surface, creating a shielding layer that prevents corrosive ions from diffusing to the metal surface.

As can be seen in Figure 5, 72 hours was the optimum immersion time. This can be supported by the corrosion rate and inhibitor efficiency data as well as the correlation with conductivity values. The corrosion rate data showed an obvious decrease within the first 24 hours following a high rate, which was then followed by stabilization. With or without inhibitors, both samples showed comparable corrosion rates after 72 hours, indicating the steady-state protective effect of the inhibitors. Even though the inhibitors' initial efficiency was high, there was a decrease over time. Nevertheless, the inhibitors performed quite well even after 72 hours of exposure, demonstrating their ability to provide better corrosion protection even after 24 hours of exposure.

As shown in Figure 6, it is evident that the rate of corrosion in all samples was initially higher as the inhibitor had not yet formed a protective layer within the first few hours. Beyond approximately 40 hours, the corrosion rate stabilized and showed minimal change up to 72 hours. The inhibitor efficiency dropped steadily over time for all samples, with the most significant decrease occurring in the first few hours. The inhibitor performance improved after about 40 hours and remained mostly unchanged for the next 72 hours. The highest inhibitor efficiencies at 72 hours of immersion were 15.41 % observed for PANI-OA 0.1 M, followed by PANI-OA 0.08 M (12.26 %), PANI-SA 0.1M (11.24 %), and lastly PANI-SA 0.08 M with 10.06 %. All these results were below 50 % which may be due to strong interactions between the dopant and the polymer, causing changes in PANI's chemical and physical properties [14].

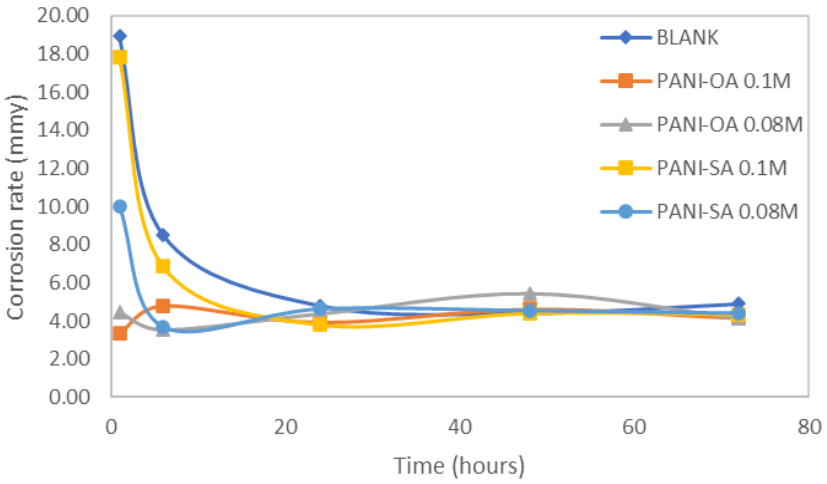

Figure 6. Corrosion rate vs. immersion time for all samples.

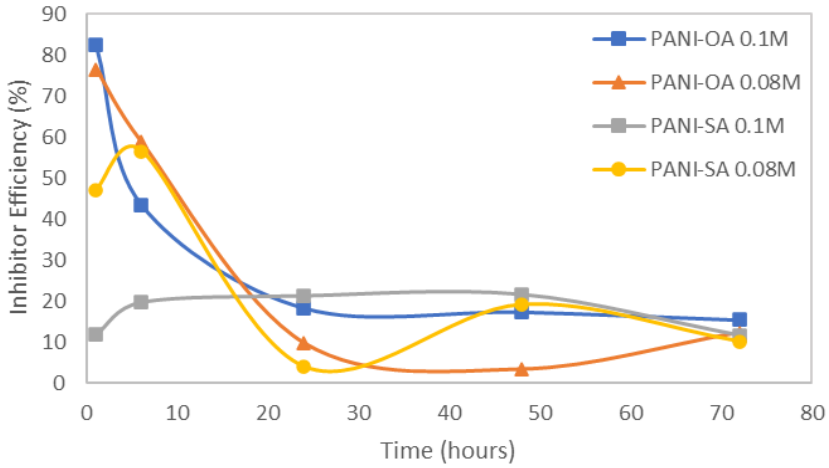

Figure 7. Inhibitor efficiency vs. immersion time for all samples.

Table 4. Weight loss parameters for all conditions in 0.5 M HCl solution.

Immersion time (hours)	Parameter	BLANK	PANI-OA 0.1 M	PANI-OA 0.08 M	PANI-SA 0.1 M	PANI-SA 0.08 M
	WL (g)	0.0017	0.0003	0.0004	0.0015	0.0009
1	CR (mmy)	18.92	3.34	4.45	17.81	10.02
	IE (%)	-	82.35	76.47	11.76	47.05
	WL (g)	0.0046	0.0026	0.0019	0.0037	0.0020
6	CR (mmy)	8.53	4.82	3.52	6.86	3.71
	IE (%)	-	43.48	58.70	19.57	56.52
	WL (g)	0.0104	0.0085	0.0094	0.0082	0.0100
24	CR (mmy)	4.82	3.94	4.36	3.80	4.64
	IE (%)	-	18.27	9.62	21.15	3.85
	WL (g)	0.0242	0.0200	0.0230	0.0190	0.0196
48	CR (mmy)	4.43	4.64	5.43	4.41	4.55
	IE (%)	-	17.36	3.31	21.49	19.00
	WL (g)	0.0318	0.0269	0.0279	0.0281	0.0286
72	CR (mmy)	4.92	4.16	4.13	4.34	4.42
	IE (%)	-	15.41	12.26	11.64	10.06

In short, 72 hours was an ideal period to analyse the inhibitors' long-term effectiveness without experiencing a major loss of their properties. In addition, the conductivity values obtained in the study support the chosen duration of 72 hours. These values were also correlated with inhibitor performance and rate of corrosion. These measurements were consistent with the corrosion rate and weight loss data. Lastly, immersion for 72 hours created a comprehensive examination of corrosion inhibition under prolonged exposure environments.

Electrochemical Impedance Spectroscopy Studies

EIS measurements provide additional details about the processes taking place at the solution or metal interface and the electrochemical frequency performance of the system. The EIS study was used to evaluate the nature of the electrochemical processes of PANI-OA and PANI-SA on the metal interface when exposed to a 0.5 M HCl solution. Figures 8, 9, and 10 illustrate impedance curves, bode plots, and phase angle plots of mild steel immersed in 0.5 M HCl at 24 hours and 72 hours, with and without the presence of an inhibitor.

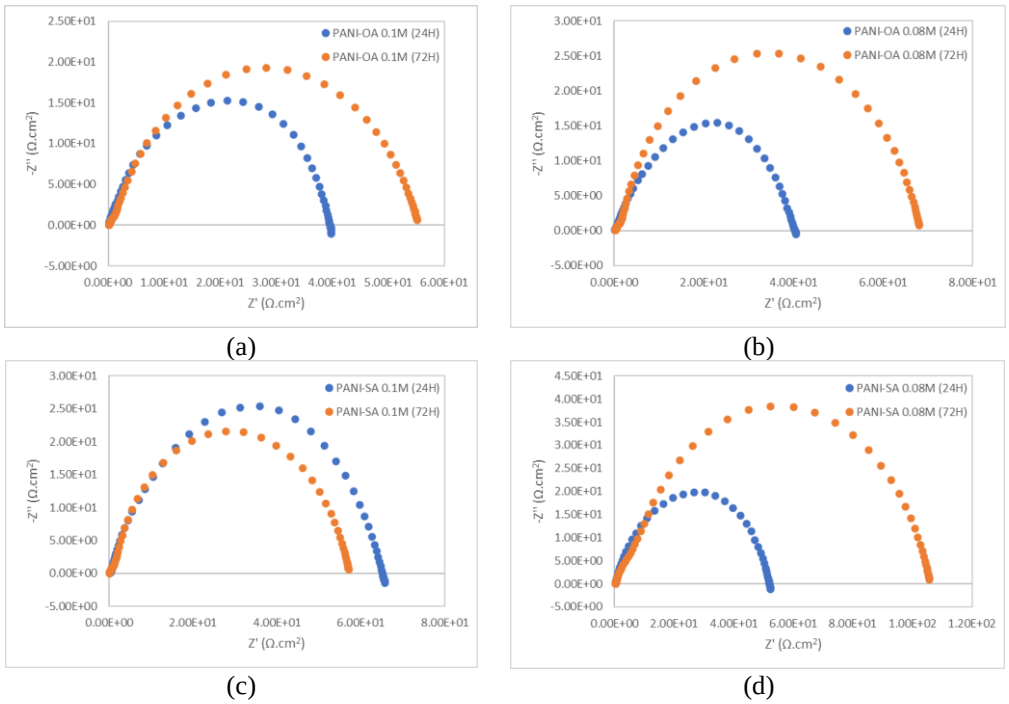

Figure 8. Nyquist plots obtained for mild steel in 0.5 M HCl with (a) PANI-OA 0.1 M, (b) PANI-OA 0.08 M, (c) PANI-SA 0.1 M, (d) PANI-SA 0.08 M.

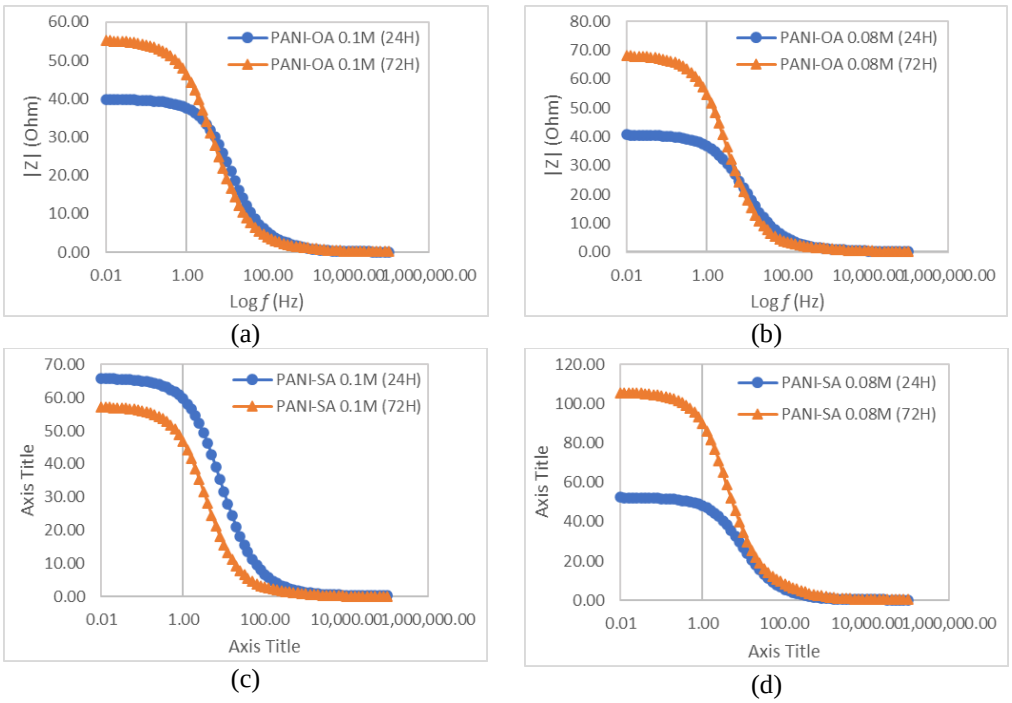

Figure 9. Bode plots obtained for mild steel in 0.5 M HCl with (a) PANI-OA 0.1 M, (b) PANI-OA 0.08 M, (c) PANI-SA 0.1 M, (d) PANI-SA 0.08 M.

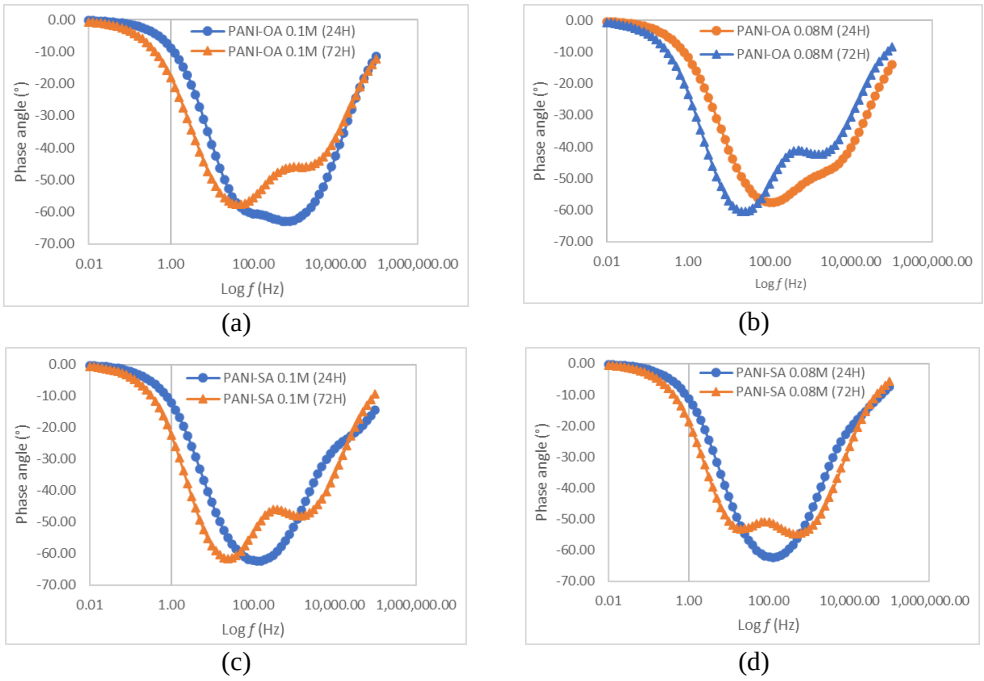

Figure 10. Phase angle plots obtained for mild steel in 0.5 M HCl with (a) PANI-OA 0.1 M, (b) PANI-OA 0.08 M, (c) PANI-SA 0.1 M, (d) PANI-SA 0.08 M.

The impedance spectra of the PANI-OA 0.1 M, PANI-OA 0.08 M, PANI-SA 0.1 M, and PANI-SA 0.08 M inhibitors are displayed in Figure 8. The mild steel samples' impedance levels changed after being submerged in the inhibitor solution for 24 and 72 hours. The results show that the protective properties of PANI OA and PANI SA changed with immersion time [15]. The diameter of a Nyquist plot is commonly used as an indicator for charge transfer resistance. A larger semicircle indicates higher charge transfer resistance, suggesting better corrosion protection.

Figure 8 shows the results for mild steel samples submerged in a 0.5 M HCl solution in the presence of PANI-OA 0.1 M, PANI-OA 0.08 M, PANI-SA 0.1 M, and PANI-SA 0.08 M as inhibitors. Most of the samples

showed larger semicircles at 72 hours compared to 24 hours. This increase in impedance after 72 hours suggests that the polyaniline inhibitors became more effective as a barrier over time, possibly due to the formation of a passive oxide layer on the metal surface, which contributed to higher charge transfer resistance. However, for PANI-SA 0.1 M, the impedance at 72 hours was lower compared to 24 hours, whereas for PANI-OA 0.1 M, the impedance at 72 hours was higher. Initially, at 24 hours, the PANI-SA 0.1 M inhibitor may have had a high level of doping, resulting in low impedance due to good conductivity. Over time, at 72 hours, the strongly acidic environment could lead to degradation, over-oxidation, or increased porosity, reducing the protective properties of the inhibitor and thus lowering impedance. Conversely, for PANI-OA 0.1 M, the initial doping level at 24 hours may be moderate, providing a balance between conductivity and stability. After 72 hours, the formation of stable complexes and the milder interaction with the PANI matrix could enhance long-term stability and barrier properties, leading to increased impedance as the coating continued to effectively protect the underlying metal. This is likely to have improved the lifespan and efficiency of the oxide layer due to the ultimate conductivity of PANI-OA.

The difference in impedance behaviour between PANI doped with 0.1 M and 0.08 M sulfuric acid over 24 and 72 hours can be explained by the balance between the initial conductivity and the long-term stability of the inhibitors. Higher dopant concentrations may provide better initial performance but lead to faster degradation, while lower concentrations may offer more stable long-term protection [16]. Understanding these dynamics is crucial for optimizing the doping level to achieve the best performance for specific applications.

Figure 9 presents the Bode plots obtained for mild steel samples in 0.5 M HCl with PANI-OA 0.1 M, PANI-OA 0.08 M, PANI-SA 0.1 M, and PANI-SA 0.08 M as inhibitors. Similar results were achieved, as seen in the Nyquist plots. The Bode plots show how the impedance magnitude changes with frequency. A high impedance at low frequencies indicates good barrier properties. The higher impedance at low frequencies for the 72-hour data suggests enhanced barrier properties and less electrolyte penetration for PANI-OA 0.1 M, PANI-OA 0.08 M, and PANI-SA 0.08 M. However, for PANI-SA 0.1 M, the lower impedance at low frequencies for the 72-hour data suggests that higher dopant concentrations may provide better initial performance but lead to faster degradation, while lower dopant concentrations might offer more stable long-term protection. Comparing PANI-SA 0.1 M with PANI-OA 0.1 M, sulfuric acid, being a stronger acid, may initially enhance conductivity but lead to faster degradation, reducing impedance over time. In contrast, oxalic acid, being a weaker acid, may form stable complexes with PANI, enhancing the coating's long-term stability and barrier properties, resulting in increased impedance over time.

The phase angle plots obtained for mild steel in 0.5 M HCl, as shown in Figure 10, provide valuable insights into the capacitive behaviour of the inhibitors. In all samples, the obtained phase angle diagrams showed one capacitive loop after 24 hours, except for PANI-OA, and two capacitive loops after 72 hours. Hence, the obtained data demonstrated a time-dependent change in inhibitor properties. In addition, the phase angle values increased with an increase in inhibitor concentration, implying that the capacitive properties of the inhibitor improved with longer usage. At higher frequencies, the capacitive loop mirrored the naturally formed protection layer. However, at lower frequencies, it correlated to the charge transfer reaction. This observation is supported by the simulated equivalent circuits used to fit the Electrochemical Impedance Spectroscopy (EIS) data, as depicted in Figures 11 and 12. The equivalent circuit components include R_s (electrolyte resistance), C_{film} (capacitance of the film), R_{film} (resistance of the film), C_{dl} (double layer capacitance), and R_{ct} (charge transfer resistance). The EIS data values are comprehensively presented in Table 4.4, providing a detailed quantitative assessment of the impedance characteristics that supports the qualitative observations from the phase angle plots.

The equivalent circuit seen in Figure 11 was used to fit the EIS data for the blank sample. The solution resistance (R_s), constant phase element (CPE), and charge transfer resistance (R_{ct}) were the three main parts of this circuit. The solution resistance represents the resistance of the electrolyte solution, whereas the CPE simulates the non-ideal capacitive behaviour of the electrochemical double layer. The charge transfer resistance, which reflects the rate of corrosion, shows the resistance to electron transfer across the metal-electrolyte interface.

As shown in Figure 12, mild steel with inhibitors required a more complicated equivalent circuit for fitting EIS data. There were two constant phase elements (CPE) in this circuit in addition to the solution resistance (R_s) and film resistance (R_f). Film resistance is a measure of the protective inhibitory film's resistance that forms on a metal surface. This circuit also had a charge transfer resistance (R_{ct}); however, the presence of inhibitors usually caused this value to increase, indicating a lower rate of corrosion. Kong et al. (2019) stated that non-idealistic factors like surface roughness, inhibitor adsorption, and the development of porous layers made it impossible to accurately simulate the impedance response without the use of CPEs in these circuits [17]. Inhibitors play a crucial role in preventing mild steel from corroding in an acidic environment, as shown by the clear differences in impedance characteristics between the two circuits.

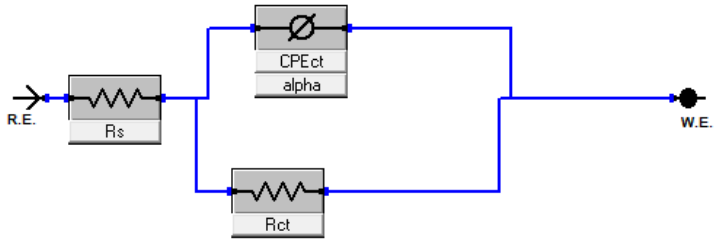

Figure 11. The equivalent circuit used to fit EIS data for mild steel in 0.5 M HCl.

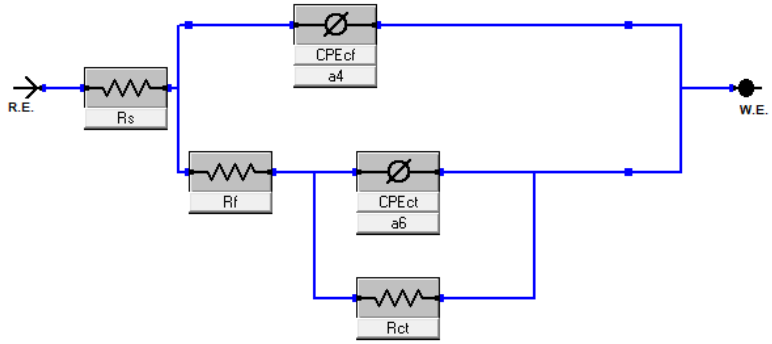

Figure 12. The equivalent circuit used to fit EIS data for mild steel with inhibitors in 0.5 M HCl.

Tables 5 and 6 show that the impedance data of the two acid dopants (PANI-OA and PANI-SA) varied significantly when compared at 0.1 M and 0.08 M. The charge transfer resistance (R_{ct}) values of the PANI-SA samples were higher than those of the PANI-OA samples after being submerged in 0.5 M HCl for 24 hours. The R_{ct} values of PANI-SA 0.1 M and PANI-SA 0.08 M after 24 hours of immersion were 65.21 Ω.cm² and 51.76 Ω.cm², respectively. This shows that PANI-SA provided excellent short-term corrosion protection. PANI-SA 0.08 M exhibited better performance over a 72-hour immersion, with the highest R_{ct} value of 86.38 Ω.cm², indicating enhanced long-term protection. All samples had relatively low solution resistance (R_s) values, but PANI-SA 0.08 M had the highest value over time, reaching 472.2×10^{-3} Ω.cm², which is indicative of the formation of a more resistive film. The presence of inhibitors increased the constant phase element (CPE_{cf}) values, which indicate changes in double-layer capacitance caused by inhibitor adsorption.

Measurements of conductivity were consistent with these results, where PANI doped with sulfuric and oxalic acids exhibited higher conductivity values, especially at higher concentrations. The conductivity and impedance data were also consistent with the weight loss analysis. Reduced weight loss is an indication of improved inhibitor efficiency, which was achieved with PANI doped with higher concentrations of acids.

Table 5. Impedance parameters for mild steel after 24 hours of immersion in 0.5 M HCl.

Parameter	PANI-OA 0.1 M	PANI-OA 0.08 M	PANI-SA 0.1 M	PANI-SA 0.08 M
R_s (Ω•cm²)	114.8×10^{-3}	143.9×10^{-3}	253.1×10^{-3}	333.2×10^{-3}
R_{ct} (Ω•cm²)	24.79	38.47	65.21	51.76
CPE_{cf} (F/cm2)	898.5×10^{-6}	860.2×10^{-6}	210.0×10^{-6}	574.8×10^{-6}
CPE_{ct}	145.3×10^{-6}	661.0×10^{-6}	685.4×10^{-6}	398.5×10^{-6}
IE%	78.18	66.16	42.60	54.44

Table 6. Impedance parameters for mild steel after 72 hours of immersion in 0.5 M HCl.

Parameter	PANI-OA 0.1 M	PANI-OA 0.08 M	PANI-SA 0.1 M	PANI-SA 0.08 M
R_s (Ω•cm^2)	172.1×10^{-3}	248.6×10^{-3}	152.3×10^{-3}	472.2×10^{-3}
R_{ct} (Ω•cm^2)	52.30	65.24	54.20	86.38
CPE_{cf} (F/cm2)	1.092×10^{-3}	980.7×10^{-6}	1.201×10^{-3}	574.8×10^{-6}
CPE_{ct}	715.8×10^{-6}	790.4×10^{-6}	755.8×10^{-6}	398.5×10^{-6}
IE%	35.30	19.29	32.95	6.90

CONCLUSION

In a nutshell, this study examined how doping polyaniline (PANI) with different acids influenced both its conductivity characteristics and its ability to prevent mild steel from corroding in acidic environments. The disappearance of the N-H signal for aniline in the FTIR spectra of doped PANI suggests polymerization of the conductive polymer had occurred. The peak at 1060-1080 cm^{-1} indicated the presence of a dopant in the PANI structure. Higher concentrations and pH values contributed to higher conductivity for doped PANI samples, where PANI-OA 0.01 M had a conductivity value of 330×10^{-3} S/cm (pH of 4.39), while PANI-SA 0.01 M had a conductivity value of 1.015×10^{-3} S/cm (pH 3.60). The optimum immersion time of 72 hours was obtained from the weight loss data in combination with conductivity values and corrosion rate data. PANI-OA 0.1 M showed higher inhibitor efficiency (15.41 %) in the weight loss analysis than PANI-OA 0.08 M (12.26 %). The sample that displayed the highest conductivity was PANI doped with oxalic acid at the highest concentration (0.1 M). These results show that acid-doped PANI has great potential as a mild steel corrosion inhibitor in acidic environments due to its higher conductivity and better porous structure. However, the concentration and type of acid used greatly influenced the electrochemical behaviour of the samples.

ACKNOWLEDGEMENTS

The authors would like to acknowledge Universiti Teknologi MARA for providing designated labs and facilities for the research.

REFERENCES

1. Shah, A. & Ul Haq, A. (2022) Corrosion Inhibition Properties of Sulfonated Polyaniline-Poly (Vinyl Alcohol) Composite on Mild Steel. *J. Chem. Chem. Eng. Research Article*, **41(4)**.

2. Palanisamy, G. (2019) Corrosion Inhibitors (A. Singh, Ed.). *IntechOpen*. https://doi.org/10.5772/intechopen.76742.

3. Lu, Y., Feng, H., Xia, H. & Xia, W. H. (2022) Carboxymethyl Cellulose-Polyaniline composites as efficient corrosion inhibitor for Q235 steel in 1 M HCl solution. *International Journal of Electrochemical Science*, **17**. https://doi.org/10.20964/2022.11.69.

4. Rahayu, I., Eddy, D. R., Novianty, A. R., Rukiah, Anggreni, A., Bahti, H. & Hidayat, S. (2019) The effect of hydrochloric acid-doped polyaniline to enhance the conductivity. *IOP Conference Series: Materials Science and Engineering*, **509**, 012051. https://doi.org/10.1088/1757-899X/509/1/012051.

5. Norouzian, R. S. & Lakouraj, M. M. (2020) Polyaniline-thiacalix[4]arene metallopolymer, self-doped, and externally doped conductive polymers. *Progress in Organic Coatings*, **146**. https://doi.org/10.1016/j.porgcoat.2020.105731.

6. Noby, H., El-Shazly, A. H., Elkady, M. F. & Ohshima, M. (2019) Strong acid doping for the preparation of conductive polyaniline nanoflowers, nanotubes, and nanofibers. *Polymer*, **182**. https://doi.org/10.1016/j.polymer.2019.121848.

7. Rahman Md., M., Mahtab, T., Mukhlish Bin, M. Z., Faruk, M. O. & Rahman, M. M. (2021) Enhancement of electrical properties of metal-doped polyaniline synthesized by different doping techniques. *Polymer Bulletin*, **78(9)**, 5379–5397. https://doi.org/10.1007/s00289-020-03389-9.

8. Fernando, J. & Vedhi, C. (2019) Synthesis, spectral characterization, and electrochemical behavior of oxalic acid doped polyanilines. *Materials Today: Proceedings*, **48**, 174–180. https://doi.org/10.1016/j.matpr.2020.06.051.

9. Bhandari, H., Choudhary, V. & Dhawan, S. K. (2011) Influence of self-doped poly(aniline-co-4-amino-3-hydroxy-naphthalene-1-sulfonic acid) on corrosion inhibition behavior of iron in acidic medium. *Synthetic Metals*, **161(9–10)**, 753–762. https://doi.org/10.1016/j.synthmet.2011.01.026.

10. Alesary, H. F., Ismail, H. K., Khudhair, A. F. & Mohammed, M. Q. (2018) Effects of dopant ions on the properties of polyaniline conducting polymer. *Oriental Journal of Chemistry*, **34(5)**, 2525–2533. https://doi.org/10.13005/ojc/340539.

11. Lu, Y., Yu, Z., Un, H., Yao, Z., You, H., Jin, W., Li, L., Wang, Z., Dong, B., Barlow, S., Longhi, E., Di, C., Zhu, D., Wang, J., Silva, C., Marder, S. R. & Pei, J. (2020) Persistent Conjugated Backbone and Disordered Lamellar Packing Impart Polymers with Efficient n-Doping and High Conductivities. *Advanced Materials*, ***33*(2)**. https://doi.org/10.1002/adma.202005946.

12. Yang, S., Yin, Q., Lian, J., Li, G., Wei, Y. & Zhu, Q. (2023) Porous surface-induced growth of HCl-doped PANi flexible electrode for high-performance Zn-ion batteries with convertible storage sites. *Electrochimica Acta*, **439**, 141691. https://doi.org/10.1016/j.electacta.2022.141691.

13. Goswami, S., Nandy, S., Fortunato, E. & Martins, R. (2023) Polyaniline and its composites engineering: A class of multifunctional smart energy materials. *Journal of Solid State Chemistry*, **317**. https://doi.org/10.1016/j.jssc.2022.123679.

14. Ingle, R. V., Shaikh, S. F., Bhujbal, P. K., Pathan, H. M. & Tabhane, V. A. (2020) Polyaniline Doped with Protonic Acids: Optical and Morphological Studies. *ES Materials and Manufacturing*, **8**, 54–59. https://doi.org/10.30919/esmm5f732.

15. Yu, Q., Liu, J., Xu, J., Yin, Y., Han, Y. & Li, B. (2015) Effects of fluorine atoms on structure and surface properties of PANI and fluorinated PANI/GPTMS hybrid films. *Journal of Sol-Gel Science and Technology*, ***75*(1)**, 74–81. https://doi.org/10.1007/s10971-015-3678-4.

16. Zulkifli, N. A., Firdaus, S. M. & Mariatti, M. (2020) Properties of conductive PANI fabricated using different dopant acids and molar ratios. *AIP Conference Proceedings*, **2267**. https://doi.org/10.1063/5.0015755.

17. Kong, P., Chen, N., Lu, Y., Feng, H. & Qiu, J. (2019) Corrosion by Polyaniline/Salicylaldehyde modified chitosan in hydrochloric acid solution. International Journal of Electrochemical Science, **14(10)**, 9774–9775. https://doi.org/10.20964/2019.10.11.